Synchronization of Circadian Oscillation of Phosphorylation Level of KaiC In Vitro

Tetsuro Nagai,[†‡] Tomoki P. Terada,[†§] and Masaki Sasai[†§¶‖*]

[†]Department of Computational Science and Engineering, Nagoya University, Nagoya, Japan; [‡]Division of Biological Science, Graduate School of Science, Nagoya University, Nagoya, Japan; [§]Department of Applied Physics, Nagoya University, Nagoya, Japan; [¶]School of Computational Sciences, Korea Institute for Advanced Study, Seoul, Korea; and [‖]Okazaki Institute for Integrative Bioscience, Okazaki, Aichi, Japan

ABSTRACT In recent experimental reports, robust circadian oscillation of the phosphorylation level of KaiC has been reconstituted by incubating three cyanobacterial proteins, KaiA, KaiB, and KaiC, with ATP in vitro. This reconstitution indicates that protein-protein interactions and the associated ATP hydrolysis suffice to generate the oscillation, and suggests that the rhythm arising from this protein-based system is the circadian clock pacemaker in cyanobacteria. The mechanism of this reconstituted oscillation, however, remains elusive. In this study, we extend our previous model of oscillation by explicitly taking two phosphorylation sites of KaiC into account and we apply the extended model to the problem of synchrony of two oscillatory samples mixed at different phases. The agreement between the simulated and observed data suggests that the combined mechanism of the allosteric transition of KaiC hexamers and the monomer shuffling between them plays a key role in synchronization among KaiC hexamers and hence underlies the population-level oscillation of the ensemble of Kai proteins. The predicted synchronization patterns in mixtures of unequal amounts of two samples provide further opportunities to experimentally check the validity of the proposed mechanism. This mechanism of synchronization should be important in vivo for the persistent oscillation when Kai proteins are synthesized at random timing in cyanobacterial cells.

INTRODUCTION

Many organisms exhibit circadian rhythms to adapt to the daily change of earth's environment. A simplest organism among them is the cyanobacterium *Synechococcus elongatus*, in which the gene cluster *kaiABC* and its product proteins KaiA, KaiB, and KaiC are essential for generating the rhythm (1). It has been observed that KaiC regulates expression of *kaiB* and *kaiC* (1,2), which conforms to the widely accepted notion that circadian oscillation is generated by dynamical feedback regulation of gene expression (3). The experiment of Kondo and colleagues (4), however, provides a strong counterexample to this notion. These authors observed robust circadian oscillation of the phosphorylation level of KaiC by incubating KaiA, KaiB, and KaiC with ATP in vitro, which indicates that interactions among Kai proteins and the associated ATP hydrolysis suffice to generate the circadian rhythm. The mechanism of oscillation in this protein-only system, however, remains elusive.

Intensive experimental observations have been made on structures and reactions of Kai proteins (5–25). KaiC forms hexamers in solution (11,12,24,25), and KaiC hexamers are phosphorylated when the solution mixture of KaiC and KaiA is incubated with ATP, showing that KaiA catalyzes phosphorylation of KaiC (8,9). KaiB binds to KaiC to attenuate the activity of KaiA, which promotes dephosphorylation of KaiC (7,23–25). The solution mixture of KaiA, KaiB, and KaiC shows the oscillation with two alternating phases: in the phosphorylation phase, KaiC is phosphorylated through interactions with KaiA, whereas in the dephosphorylation phase, KaiB has the higher affinity to KaiC to attenuate the activity of KaiA (7,25). Thus, the affinity of KaiA or KaiB to KaiC depends on the phosphorylation level of KaiC, which constitutes the basis for the mechanism of oscillation.

There are two major questions concerning this basic picture of oscillation. The first regards the mechanism of persistent oscillation of individual KaiC hexamers. Each KaiC monomer has two residues, Ser^{431} and Thr^{432}, which are phosphorylated and dephosphorylated in a definite order. When we write the phosphorylated and dephosphorylated Ser^{431} as pSer and Ser and the phosphorylated and dephosphorylated Thr^{432} as pThr and Thr, respectively, the sequence of changes in the phosphorylation state, Ser/Thr → Ser/pThr → pSer/pThr → pSer/Thr → Ser/Thr, was observed in every cycle of oscillation (26,27). Since both Ser^{431} and Thr^{432} are located near the ATP-binding site (10), we should expect that each KaiC hexamer undergoes the structural change to facilitate the coordinated reactions including ATP hydrolysis (28) and phosphorylation/dephosphorylation of Thr and Ser, which should be correlated to the change in the binding affinity of KaiA or KaiB to KaiC (29). The atomistic picture of such coordinated action of structural change is needed to elucidate the mechanism of oscillation from the microscopic viewpoint.

The second important question regards how oscillations of a large number of KaiC hexamers are synchronized. Even when individual KaiC hexamers oscillate through the definite sequence of the state change, the averaged phosphorylation level of many KaiC hexamers does not show a distinct

Submitted October 22, 2009, and accepted for publication February 26, 2010.

*Correspondence: sasai@nuap.nagoya-u.ac.jp

Editor: Andre Levchenko.

0006-3495/10/06/2469/9 $2.00

doi: 10.1016/j.bpj.2010.02.036

oscillation if the oscillatory phase of many KaiC hexamers is randomly distributed. The observed clear oscillation of the in vitro system (4,25) shows that many KaiC hexamers are indeed synchronized to have the same oscillatory phase. We here call this synchronization molecular synchronization. Although these two problems, the oscillation of individual KaiC hexamers and molecular synchronization, should be interrelated to each other, we separate them below for the sake of discussion.

The problem of molecular synchronization has been the focus of theoretical studies (27,30–40). We here categorize the hitherto proposed theoretical models into four types. 1), Feedback through complex formation. A simplest possible assumption is that KaiC hexamers can communicate with each other through direct interactions to form complexes of KaiC hexamers (30,31). When the phosphorylated KaiC catalyzes phosphorylation of the less phosphorylated KaiC through such direct interactions, for example, the positive feedback loop is formed, which synchronizes the oscillatory phase of KaiC hexamers. This idea can be extended by assuming that KaiC-KaiC interactions are mediated by KaiA or KaiB (32,33). Although these assumptions can mathematically give rise to synchronization, there is no experimental evidence to support such direct interaction or KaiA- or KaiB-mediated interaction between KaiC hexamers (25), and hence we do not pursue this line further in this article. 2), Autocatalytic inhibition of the reverse reaction. Three assumptions were made in this type of model (27,34): a), the net flow of pSer/pThr → pSer/Thr is slow, because KaiA catalyzes the reverse reaction pSer/pThr ← pSer/Thr, so that KaiC accumulates at the pSer/pThr state; b), KaiB does not bind to pSer/pThr but does bind to pSer/Thr; and c), the KaiBC complex formed in the pSer/Thr state inhibits the activity of KaiA by forming the KaiABC complex. With these assumptions, KaiC hexamers accumulated in the pSer/pThr state are collectively transformed to the pSer/Thr state due to the autocatalytic inhibition of the pSer/pThr ← pSer/Thr reaction. The collective transformation of pSer/pThr → pSer/Thr can thus synchronize the oscillatory phase of KaiC. However, all three of the above assumptions contradict the experimental observations on phosphomimetic mutants of KaiC (26,34). When mutations at Ser^{431} or Thr^{432} are considered to mimic the change in the phosphorylation state, then a′) the autophosphatase reaction pSer/pThr → pSer/Thr is fast, and the rate is not affected by the presence or absence of KaiA or KaiB; b′) KaiB binds to both pSer/pThr and pSer/Thr with similar binding affinity; and c′) KaiB inhibits the reaction pSer/Thr ← Ser/Thr but does not inhibit other reactions significantly. 3), Depletion of free KaiA or KaiB. The assumption of depletion of KaiA or KaiB leads to the other type of scenario of synchronization (35,36). van Zon, Lubensky, Altena, and ten Wolde (ZLAW) (36) assumed that the binding affinity of KaiA to KaiC depends on the phosphorylation level of KaiC. Then, the stronger tendency to form the KaiAC complex at some phosphorylation levels may lead to a shortage of free KaiA in solution. This shortage inhibits phosphorylation of KaiC at the other levels of phosphorylation, leading to an accumulation of KaiC at those phosphorylation levels, which synchronizes the oscillation. It has been pointed out that the assumption of depletion of KaiA should lead to the prediction that the oscillation is sensitively weakened when concentration of KaiA in solution is increased (36–38). Experimental examination of the predicted fragility of oscillation against increase in the KaiA concentration can be a test of the ZLAW scenario. 4), Monomer shuffling. It has been experimentally shown that KaiC hexamers exchange monomers among themselves (25,39,41). Yoda, Eguchi, and colleagues (37,38) and Mori et al. (39) showed that oscillations are synchronized when this monomer shuffling works with the allosteric transition of KaiC hexamers.

The model of allosteric transition and monomer shuffling (AMS) proposed here explains many of the data observed in the Kai protein system (37,38). It has been experimentally observed that the oscillation is persistent when concentrations of Kai proteins are increased from those used in the standard experimental setup, but that the oscillation dies out when the concentrations are decreased to 1/10 or less of those concentrations (25). It has also been observed that under the condition of the fixed concentration of KaiC at its standard value, the oscillation dies out when the KaiA concentration is decreased to 1/4 or the KaiB concentration to 1/3 of standard values (25). These observed features were well reproduced by the AMS model (37,38). It was experimentally observed (25) that the concentration of free KaiC oscillates 180° out of phase with the concentration of KaiBC complex and in phase with that of KaiAC complex, which is also explained by the AMS mechanism (37). The simulated kinetics of formation of KaiAC or KaiBC complex and the simulated kinetics of monomer shuffling (37) were consistent with the observed data (25). The AMS model further predicts that the oscillation will be robust against an increase in the concentration of KaiA (38). It is necessary to further check the dependence of oscillation on the systematic stoichiometric change of Kai proteins.

Emberly and Wingreen (40) also argued that monomer shuffling helps synchronization, but their model was based on two assumptions, that KaiC hexamers gather to form clusters of mesoscopic size, which inhibits phosphorylation during the dephosphorylation period, and that monomer shuffling is most frequent when KaiC hexamers are isolated from clusters in the phosphorylation period. However, these two assumptions contradict experimental observation: no stable cluster of KaiC hexamers was observed in vitro (25), and the frequency of monomer shuffling is greatest in the early stage of the dephosphorylation period (25,41).

It is thus apparent that not all models fit the existing experimental data, and to find whether there is a correct theoretical scenario among those proposed, the remaining models have to be critically checked by further experimental tests. Here, we focus on the recent experiments in which two samples

are mixed. When two in vitro oscillator samples at different phases are mixed together, the sample mixture shows a stable oscillation with a phase that often approximates either of the two sample phases before mixing (41). We call this oscillator synchronization. Since oscillator synchronization should directly reflect the mechanism of molecular synchronization, it can be a critical test for examining scenarios of molecular synchronization. We thus examine in this article whether the AMS model explains the observed data of oscillator synchronization.

Since recently observed dual phosphorylation at two phosphorylation sites, Ser^{431} and Thr^{432}, in KaiC characterizes the oscillation phase more precisely, we here treat the phosphorylation of both Ser^{431} and Thr^{432}, instead of treating only phosphorylation of Ser^{431}, as in our previous AMS model (37,38). We thus modify our previous single-phosphorylation-site models by explicitly taking account of both phosphorylation sites. Precise modes of interaction between KaiA and KaiC and between KaiB and KaiC were discussed in our previous AMS model study to examine the dependence of oscillation on concentrations of KaiA and KaiB (37,38). In this article, however, we focus on oscillator synchronization and do not consider changes in concentration of KaiA or KaiB, thus implicitly taking account of KaiA and KaiB only. The AMS model is explained in detail in the subsection Allosteric transition and monomer shuffling, and the oscillation in the AMS model is explained in the subsection Oscillation patterns. The simulated results of synchronization in sample mixtures are then discussed in the subsection Oscillator synchronization. Details of the model are described in Text S1 in the Supporting Material.

RESULTS

Allosteric transition and monomer shuffling

Although phosphorylation and dephosphorylation phases in the oscillatory system have been discerned experimentally (25–28), it has not yet been clarified what molecular features of KaiC distinguish these two phases. A reasonable assumption one can make is that the two phases are characterized by two different structural states of KaiC. The two-state structural change of the KaiC hexamer may be brought about through interactions among monomers in a way similar to the allosteric transition of hemoglobin (42,43) or chaperonin (44,45). We thus assume the allosteric transition as shown in Fig. 1 *a*. We refer to two allosteric states of the KaiC hexamer as tense (T) and relaxed (R) states. Since monomer shuffling is more frequent in the dephosphorylation phase (25) and should take place when the hexamer structure is somewhat loosened in the R state, it is reasonable to regard KaiC as in the R state in the dephosphorylation phase and in the T state in the phosphorylation phase. The assumption of allosteric transition is consistent with the observed alternation of two phases when the affinity of KaiB to KaiC is

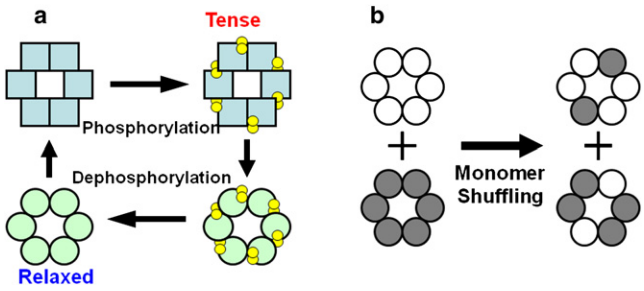

FIGURE 1 Allosteric transition and monomer shuffling. (*a*) Allosteric transition of the KaiC hexamer between tense (T) and relaxed (R) structures is assumed in the model. Monomers in the T hexamer and those in the R hexamer are illustrated with squares and circles, respectively, and phosphorylated sites are illustrated with yellow circles. KaiB is assumed to have a higher affinity to KaiC in the R structure, so that KaiB attenuates the action of KaiA when KaiC is in the R state. Hence, KaiA promotes the autokinase reaction of KaiC in the T state, and KaiC in the R state is dephosphorylated by the autophosphatase reaction of KaiC. The transition from T to R is assumed to take place with higher frequency when T is more phosphorylated, and the transition from R to T is assumed to take place with higher frequency when R is less phosphorylated. With these assumptions, we can expect that each KaiC hexamer cyclically repeats phosphorylation and dephosphorylation, but communication among many KaiC hexamers is necessary to sustain coherent oscillation of the meso- or macroscopic sample solution. (*b*) A candidate mechanism of communication between KaiC hexamers is the exchange of monomers between KaiC hexamers, i.e., monomer shuffling.

higher for KaiC in the R state. The higher affinity of KaiB should then attenuate the action of KaiA in the R state, which enhances the autophosphatase reactions of KaiC. Phosphorylation and dephosphorylation should proceed sequentially, as observed in experiments (25,26), when the transition $T \rightarrow R$ is more frequent in KaiC at the higher phosphorylation level and the transition $R \rightarrow T$ is more frequent in KaiC at the lower phosphorylation level. With these assumptions summarized in Fig. 1 *a*, it is evident that individual KaiC hexamers exhibit oscillation in the phosphorylation level. Verification of these assumptions in terms of molecular structure remains an important open problem, but by admitting these assumptions as a working hypothesis, we can proceed to the problem of molecular synchronization. Similar assumptions on allosteric transition were made in the Mori et al. (39) and ZLAW (36) models.

Molecular synchronization in the AMS model is realized through monomer shuffling of KaiC. As monomer shuffling should be more frequent in the R state than in the T state (25), we here ignore the less frequent monomer shuffling between KaiC hexamers in the T state and consider the shuffling reactions $R + R \rightarrow R + R$ (Fig. 1 *b*). Since monomer shuffling is most frequent in the beginning of the dephosphorylation period (25), we consider that the highly phosphorylated R state has the additional channels of shuffling reactions $T + R \rightarrow R + R$. Here, it is assumed that the two KaiC hexamers after shuffling are in the R state, because the structure just after shuffling should be more destabilized than the structure

before shuffling. We note that the reactions T + R→R + R lead to a nonlinear increase of R: when the allosteric transition T→R is not so fast, KaiC hexamers accumulate in the T state at the highly phosphorylated level. These accumulated KaiC hexamers are collectively transformed to the R state through the autocatalytic reactions T + R→R + R, which synchronizes the oscillatory phase of KaiC hexamers. Synchronization through monomer shuffling was also argued by Mori et al. (39), but in their model, only the shuffling reactions R + R→R + R and T + T→T + T were assumed, and the reactions T + R→R + R were prohibited, whereas the reactions T + R→R + R have key importance in the AMS mechanism presented here.

In this article, KaiC hexamers are denoted by $T_{i,j}$ or $R_{i,j}$, where T and R represent the structural states; i is the number of phosphorylated Ser^{431} residues in the hexamer, with $0 \le i \le 6$; and j is the number of phosphorylated Thr^{432} residues in the hexamer, with $0 \le j \le 6$. To focus on the phenomena of oscillator synchronization, we take account of KaiA and KaiB only implicitly by imposing the constraints that phosphorylation reactions proceed in the T state and dephosphorylation reactions proceed in the R state. Fig. 2 illustrates the whole reaction scheme in the version of the model presented in this article. Here, we coarse-grained the model by skipping some reaction steps, as described in Text S1 in the Supporting Material. To examine whether the oscillator synchronization in the model is robust against stochastic fluctuations in reactions, we numerically simulated the reactions in the model with the Gillespie algorithm (46). See Text S1 in the Supporting Material for further details on the model.

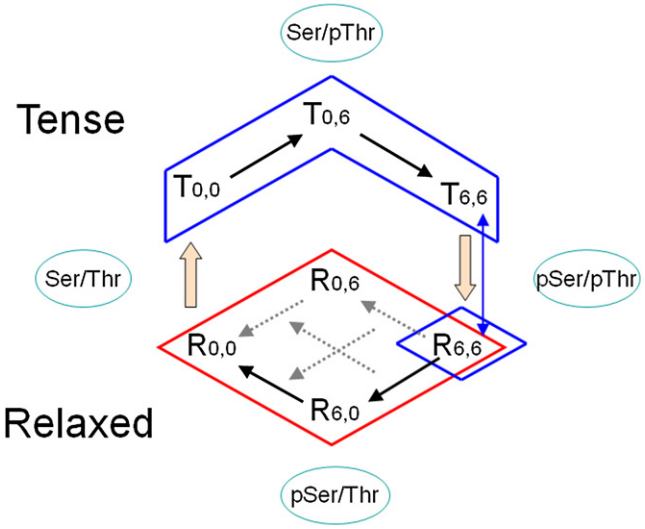

FIGURE 2 Scheme of reactions in the model. KaiC hexamer undergoes a sequence of phosphorylation and dephosphorylation as Ser/Thr→Ser/pThr→pSer/pThr→pSer/Thr→Ser/Thr. The KaiC hexamer in the T state and the KaiC hexamer in the R state with i sites of phosphorylated Ser^{431} and j sites of phosphorylated Thr^{432} are designated by $T_{i,j}$ and $R_{i,j}$, respectively. KaiC hexamers in the R state (*red-outlined area*) and those in the T state and $R_{6,6}$ (*blue-outlined areas*) are assumed to exchange monomers within an area outlined in the same color. Allosteric transition is indicated by the pink arrows.

Oscillation patterns

With the parameters and rate constants discussed in Text S1 and Table S1 in the Supporting Material, the model presented here can reproduce the oscillation of the phosphorylation level of KaiC. The simulated phosphorylation level, $p(t)$, depicted in Fig. 3 *a*, is defined by

$$p(t) = \frac{1}{12\,N_0}\sum_{i,j}(i+j)X_{i,j}(t). \quad (1)$$

Here, $X_{i,j}(t) = N(T_{i,j}, t) + N(R_{i,j}, t)$, and $N(T_{i,j}, t)$ and $N(R_{i,j}, t)$ are numbers of KaiC hexamers in the states $T_{i,j}$ and $R_{i,j}$ at time t in the system. $N_0 = 10{,}000$ is the total number of KaiC hexamers in the simulation. As shown in Fig. 3 *a*, $p(t)$ oscillates coherently, as observed in experiments (4,25). By analyzing each simulated trajectory (Fig. 3 *b*), we can confirm that the population of KaiC hexamers oscillates according to the mechanism described in the subsection Allosteric transition and monomer shuffling. Due to the slow allosteric transition, KaiC accumulates at $T_{6,6}$. Then, $R_{6,6}$ begins to slowly increase through the allosteric transition, and when the number of KaiC at $R_{6,6}$ exceeds a certain level, the shuffling reaction between T and R becomes evident, which brings about the rapid increase of KaiC in the R state. This autocatalytic reaction induces the collective transformation of the population of KaiC hexamers from $T_{6,6}$ to $R_{6,6}$, which leads to molecular synchronization. We note that $p(t)$ in Fig. 3 *a* has an asymmetric shape: the slope of $p(t)$ in the dephosphorylation phase is steeper than that in the phosphorylation phase. Such asymmetry was indeed observed in experimental data, but to a weaker degree (41). Asymmetry was also weaker in previous versions of the AMS model (37,38), and hence, the emphasized asymmetry in Fig. 3 *a* should be due to the simplification introduced in this version of the model; neither KaiA nor KaiB is explicitly taken into account, and the reaction steps are coarse-grained, as explained in Text S1 in the Supporting Material. However, because the mechanism of molecular synchronization (Fig. 3 *b*) is the same as in the previous version of the model, we expect that the degree of asymmetry does not seriously affect the analysis of molecular and oscillator synchronizations, but rather that the model captures the essential features of those phenomena. The key importance of monomer shuffling in the model to maintain the oscillation in $p(t)$ is readily seen from Fig. 3, *c* and *d*. When monomer shuffling reactions of R + R→R + R are suppressed, the oscillation gradually damps (Fig.3 *c*). A more drastic effect is induced when the autocatalytic reactions of T + R→R + R are suppressed, which then leads to the quick damp of oscillation in $p(t)$ (Fig.3 *d*).

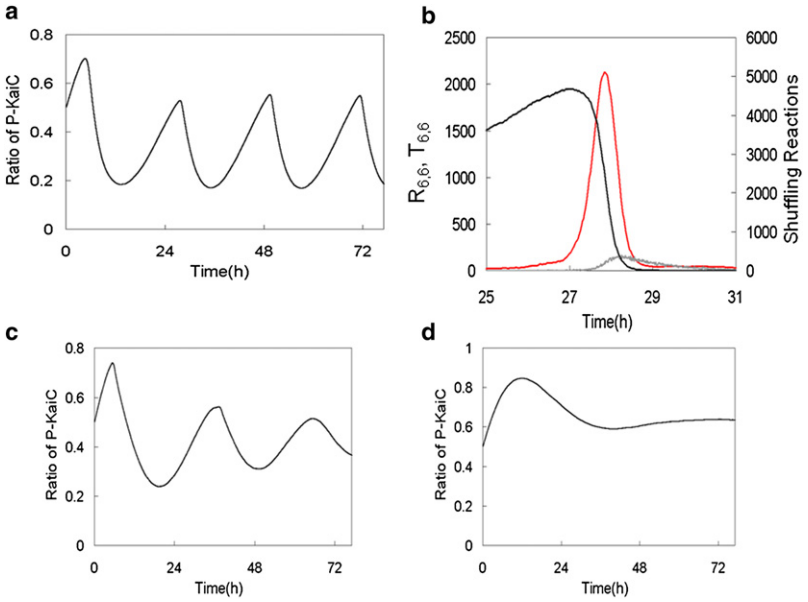

FIGURE 3 Oscillations of the system. (*a*) Simulated circadian oscillation of the ratio of phosphorylated KaiC, $p(t)$. (*b*) The numbers of $T_{6,6}$ (*black line*) and $R_{6,6}$ (*gray line*), and the frequency of monomer shuffling between T and R (*red line*) in the simulated oscillation. KaiC hexamers accumulated at $T_{6,6}$ are collectively transformed to $R_{6,6}$ through monomer shuffling. The frequency of monomer shuffling was monitored in the simulation as the number of monomer-shuffling reactions taking place during 30 min. (*c* and *d*) Oscillation is damped when shuffling reactions $R + R \rightarrow R + R$ (*c*) or $T + R \rightarrow R + R$ (*d*) are suppressed by putting $k_s^{RR} = 0$ or $k_s^{TR} = 0$, respectively, in Table S1.

The new feature of the model presented here is that the oscillations of p(Ser/Thr, t), p(Ser/pThr, t), p(pSer/pThr, t), and p(pSer/Thr, t) consistently explain the experimental data (26) as summarized in Fig. 4, where $p(\cdots, t) = n(\cdots, t)/6N_0$, and $n(\cdots, t)$ is the number of the corresponding type of KaiC monomers, and is calculated from $X_{i,j}(t)$ by assuming that i sites of phosphorylated Ser and j sites of phosphorylated Thr are distributed to monomers in each hexamer without any bias (see Text S1 in the Supporting Material). The simulated results in Fig. 4 reproduce the observed order of appearance of peaks Ser/Thr→Ser/pThr→pSer/pThr→pSer/Thr→Ser/Thr (26,27). The simulated peak heights of $p(\text{Ser}/\text{Thr}) \approx 0.7$, $p(\text{Ser}/\text{pThr}) \approx 0.4$, and $p(\text{pSer}/\text{pThr}) \approx p(\text{pSer}/\text{Thr}) \approx 0.3$ in Fig. 4 roughly agree with the experimentally observed values of $p(\text{Ser}/\text{Thr}) \approx 0.8$, $p(\text{Ser}/\text{pThr}) \approx 0.4$, and $p(\text{pSer}/\text{pThr}) \approx p(\text{pSer}/\text{Thr}) \approx 0.2$ (26).

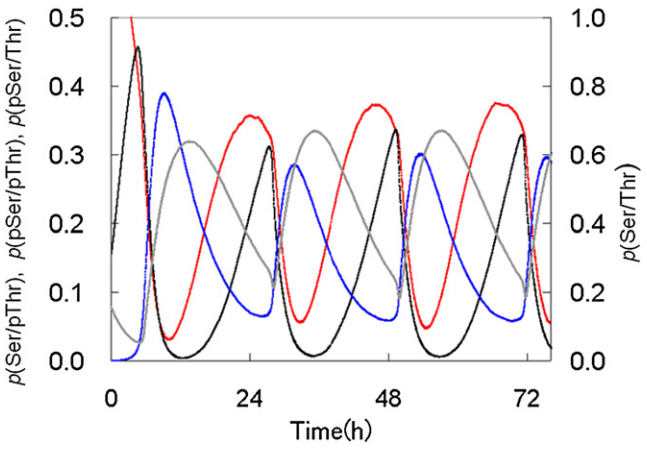

FIGURE 4 Simulated oscillation of the relative abundance of each component of KaiC hexamers, p(Ser/pThr, t) (*red line*), p(pSer/pThr, t) (*black line*), p(pSer/Thr, t) (*blue line*), and p(Ser/Thr, t) (*gray line*).

These results justify the extension of the AMS model to consider the two phosphorylation sites within individual KaiC monomers.

Oscillator synchronization

Recent experimental observation of oscillator synchronization in which two oscillating samples with different phases are mixed (41) offers further possibilities for comparison between the theoretical model and experimental results. Examples of simulated oscillator synchronization are shown in Fig. 5, *a–c*. In Fig. 5 *a*, samples at two time points of almost opposite oscillatory phases, one at phosphorylation phase B and the other at dephosphorylation phase E (Fig. 5 *d*), were mixed. A set of $N_0/2 = 5000$ KaiC hexamers was extracted from B and E by maintaining the ratios of KaiC states, $N(T_{i,j}, t)/N_0$ and $N(R_{i,j}, t)/N_0$, at each time point. These two sets of $N_0/2$ KaiC hexamers were then mixed to form a set of N_0 KaiC hexamers. If no synchronization mechanism is working in the mixture, the amplitude of the oscillation should vanish after two oscillations of opposite phases cancel each other out. Instead, however, the simulated $p(t)$ of the mixture showed a distinct oscillation entrained to the sample at time point E. A similar result is obtained in the case of mixing data at time points C and F: as shown in Fig. 5 *b*, the simulated $p(t)$ of the mixture C + F is entrained to C. These results show the strong tendency of entrainment toward the dephosphorylation phase, in agreement with experimental observation (41). However, when the sample at time B is mixed with that at E′, which is 14.5 min later than E, the sample mixture is not strongly entrained to E′ but oscillates with the phase between B and E′, as shown in Fig. 5 *c*, and hence, E is at around the boundary of the time domain to which the oscillation is entrained.

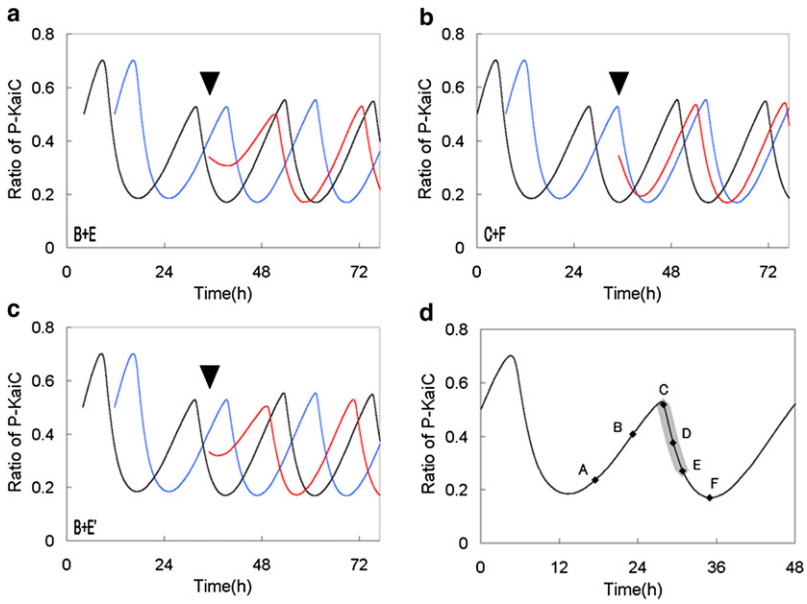

FIGURE 5 Simulated oscillator synchronization. (*a–c*) Two oscillating samples are mixed into one sample at the time designated by the black triangle. (*a*) B + E. The ratio of phosphorylated KaiC, $p(t)$, of the mixed sample (*red line*) is closer to the $p(t)$ of E (*black line*) than to the $p(t)$ of B (*blue line*). (*b*) C + F. The $p(t)$ of the mixed sample (*red line*) is closer to that of C (*blue line*) than to that of F (*black line*). (*c*) B + E′, where the phase of oscillation of E′ is 14.5 min later than that of E. The $p(t)$ of the mixed sample (*red line*) is closer to that of E′ (*black line*) than to that of B (*blue line*), but the entrainment is not so strong as in the case of B + E. (*d*) The time instances A–F at which the samples were selected before mixing. The gray area from C to E is the time duration toward which the mixed sample is strongly entrained.

We simulated mixtures of all possible pairs of the six time points from A to F (Fig. 5 *d*). The results are summarized in Fig. 6 *a*, where stochastic simulations were repeated 10 times for each mixing of samples to examine the effect of the stochastic fluctuation. Each plotted point in Fig. 6 *a* represents the time point at which the $p(t)$ of the mixture shows a peak, which is averaged over the ensemble of simulated trajectories of a mixed sample. We note that the standard deviation of peak times, δt, is typically ~0.2 h and is within the range 0.09 h $< \delta t <$ 0.49 h in every mixture in Fig. 6 *a* (the width of δt is too small to be plotted there), showing that the phase shifts in oscillator synchronization described by the AMS model are stable against stochastic fluctuation.

In Fig. 6 *a*, the vertical lines and the slanted dashed lines show the peak times of samples when two time points are unmixed. When samples at time points C, D, and E were mixed with samples at the other time points, the peak times of $p(t)$ of the mixtures clustered around the vertical line, showing that the oscillations of the mixed samples were entrained to the oscillations of the sample at time points C, D, and E. In contrast, when the samples at time points A, B, and F were mixed with samples at the other time points, the peak times of $p(t)$ of the mixtures were scattered around the slanted line, showing that the oscillations of the mixed samples were entrained to the oscillations of the other samples. In Fig. 6, the simulated data (Fig. 6 *a*) are compared

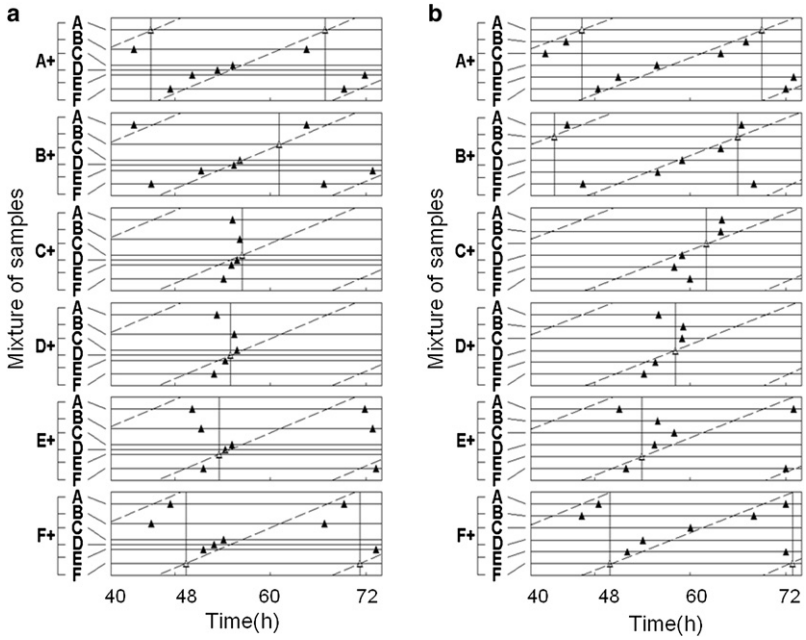

FIGURE 6 Phase shifts of each sample upon mixing with other samples shown for simulated (*a*) and observed (*b*) results. Open triangle(s) intersected by vertical line(s) in each chart represent(s) the time instance(s) at which $p(t)$ shows a peak(s) in each unmixed sample. Solid triangle(s) represents time instance(s) at which $p(t)$ shows a peak(s) in mixtures with samples listed on the left of each chart. Slanted dotted lines run through the peak times of the other samples when unmixed. Observed data were taken from Fig. 3 *c* of Ito et al. (41), with permission from the authors and from Macmillan Publishers: Nature Structural and Molecular Biology, copyright (2007).

with the experimental data (Fig. 6 *b*), which were taken from Fig. 3 *c* of Ito et al. (41). Due to the asymmetry of the simulated $p(t)$, the time durations between C and D and between D and E are narrower than other time durations in Fig. 6 *a*, but despite such differences, the distribution of plotted points in Fig. 6 *a* is remarkably similar to that in Fig. 6 *b*. Such agreement implies that the model presented here captures the essential features of oscillator synchronization observed in the experiment. Fig. S1 gives the simulated trajectories of the $p(t)$, showing the oscillator synchronization among the six time points.

Times C, D, and E are in the dephosphorylation period, and the results in Fig. 6 show that the direction of reactions in the phosphorylation period is reversed when those samples are mixed with samples at C, D, or E. Thus, the system is strongly entrained to the oscillation of the sample in the dephosphorylation phase. This can be accounted for by the common mechanism with molecular synchronization: After mixing with the sample in the dephosphorylation phase, the abundance of R state in the dephosphorylation phase increases the rate of shuffling reactions of $T + R \rightarrow R + R$, which brings KaiC hexamers in the T state to the R state. Thus, KaiC hexamers from the sample in the phosphorylation phase are entrained to the dephosphorylation phase by KaiC hexamers coming from the sample in the dephosphorylation phase by means of the allosteric transition accompanied by monomer-shuffling reactions.

By monitoring the frequency of the simulated monomer shuffling (Fig. 7 *a*), it can be verified that the same mechanism that applies in molecular synchronization indeed works in oscillator synchronization: in the B + E mixture, the frequency of monomer shuffling of $T + R \rightarrow R + R$ is high just after mixing and gradually decreases. This monomer shuffling is the necessary condition for distinct entrainment to the dephosphorylation phase and is much weaker in the B + E′ mixture, which does not exhibit strong entrainment behavior. In this way, strong entrainment is possible only toward the time domain in which monomer shuffling of $T + R \rightarrow R + R$ is frequent in the sample.

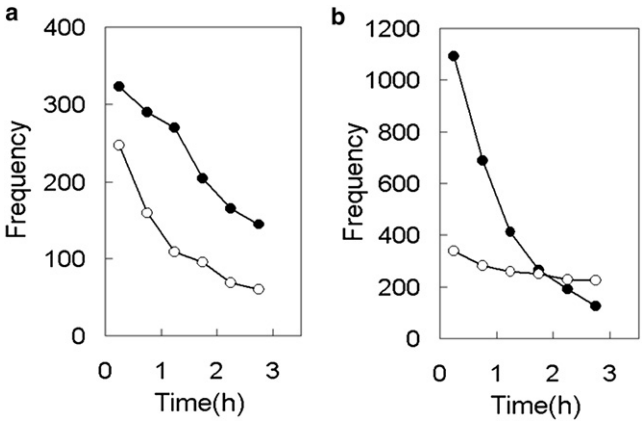

FIGURE 7 Frequency of autocatalytic monomer shuffling between KaiC hexamers. (*a*) Frequency of monomer shuffling $T + R \rightarrow R + R$ in the B + E mixture (*solid circles*) and the B + E′ mixture (*open circles*). (*b*) Frequency of monomer shuffling $T + R \rightarrow R + R$ in the C + F mixture (*solid circles*) and the C′ + F mixture (*open circles*). E′ is 14.5 min later than E, and C′ is 21 min earlier than C. The abscissa shows time elapsed after mixing. Frequency was measured as the number of monomer-shuffling reactions taking place between KaiC hexamers in the T and $R_{6,6}$ states during 30 min of simulation.

The time domain of strong entrainment is the gray area in Fig. 5 *d*. It should be noted that the boundary of this time domain is sharp in the simulated results: When we used time point C′, at 21 min before C, the mixture of C′ and F was not entrained to C′. We can confirm from Fig. 7 *b* that the monomer shuffling of $T + R \rightarrow R + R$ takes place at a much higher frequency in the C + F mixture than in C′ + F. Such a sharp change of entrainment behavior may be due to our simplification in the model. As explained in the Model section, the allosteric transition from the T to the R state was assumed to take place only through $T_{6,6} \rightarrow R_{6,6}$ in the model, but it may be able to take place through broader channels, including $T_{5,6} \rightarrow R_{5,6}$ or $T_{6,5} \rightarrow R_{6,5}$. Monomer shuffling was assumed to take place through $T_{i,j} + R_{6,6} \rightarrow R_{k,l} + R_{m,n}$, but this condition also can be broadened to allow $T_{i,j} + R_{5,6} \rightarrow R_{k,l} + R_{m,n}$, etc. By using such milder conditions, we could expect the boundary of the time domain of strong entrainment to become less sharp. Even with such modification of the model, however, the crossover of the entrainment behavior at this boundary of time domain can remain relatively distinct, and it would be interesting to examine whether such a distinct crossover is observed experimentally by moving the time points.

Fig. 8 shows how the degree of entrainment is affected by changing the mixing ratio r in the uneven mixture of two samples, referred to as samples 1 and 2, at various time points. Here, $1/(1 + r)\,N_0$ KaiC hexamers from sample 1 and $r/(1 + r)\,N_0$ KaiC hexamers from sample 2 were mixed into a sample of N_0 hexamers. In Fig. 8, *a–c*, sample 1 at times B, C, and E, respectively, was mixed with sample 2 at time instances shown on the axis of the abscissa, and the difference in peak time of $p(t)$ between the mixture and sample 1 is plotted as a contour map for various r and for various time instances of sample 2 when it was mixed with sample 1. From Fig. 8 *b*, we can see that the sample at C entrains samples at every time point as far as $r < 1.5$. For $1.5 < r < 3$, the samples at time points in a wide range are still entrained to C, showing the strength of entrainment by the sample at C. Entrainment is also strong toward the sample at E, as shown in Fig. 8 *c*, but entrainment to the sample at B is evident only for the case of $r < 0.1$, as shown in Fig. 8 *a*. These results confirm the strong entrainment to the dephosphorylation phase seen in Figs. 5 and 6. These predicted entrainment patterns in uneven mixtures can be examined by experiment, which should provide further tests to check the validity of the proposed AMS mechanism.

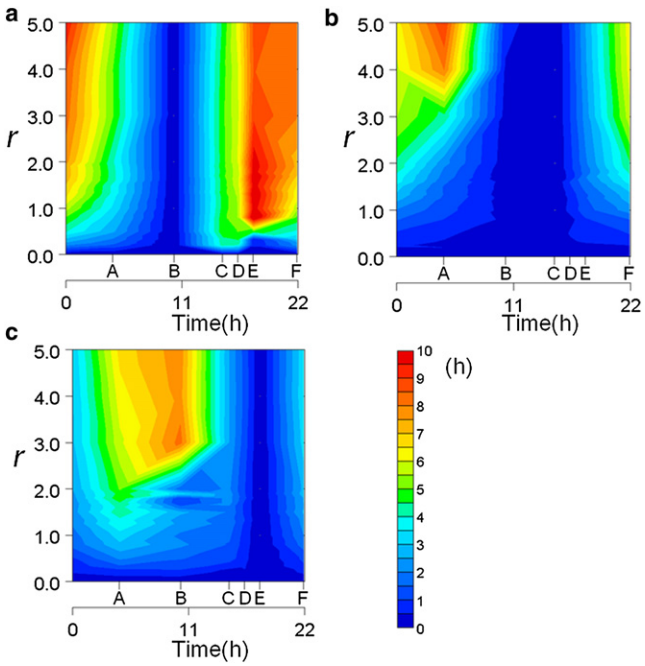

FIGURE 8 Degree of entrainment in mixtures of unequal amounts of two samples. Samples 1 and 2 were mixed at a ratio of the number of KaiC hexamers of 1:r. Degree of entrainment is expressed by the absolute difference between the peak times, $p(t)$, of sample 1 and the mixture sample, plotted as a contour map on the two-dimensional space of r and the time instances of sample 2 when it was mixed with sample 1. Sample 1 was selected at B (*a*), C (*b*), and E (*c*) of Fig. 5 *d* when it was mixed with sample 2.

DISCUSSION

In this article, we show a remarkable coincidence between the distributions of peak positions of mixed samples in the simulated results (Fig. 6 *a*) and the experimental data (Fig. 6 *b*). This accordance should imply that the combined mechanism of the accumulation of KaiC population at $T_{i,j}$ with large i and j and the collective shift of population from this accumulated state to $R_{i,j}$ gives rise to oscillator synchronization, and that the AMS mechanism explains such accumulation and collective shift of population: Accumulation at $T_{i,j}$ arises from the slow allosteric transition from T to R, and the collective shift of population is realized by the autocatalytic monomer shuffling between T and R.

We note, however, that accumulation and collective shift of population could also result from mechanisms other than the AMS mechanism. This unproved possibility should be studied through a critical check of theoretical models. As a first step, it is meaningful to examine other models from the viewpoint of how the accumulation and collective shift of population are defined in those models. In the ZLAW model (36), for example, the stronger affinity of KaiA to KaiC at the early stage of the phosphorylation period leads to accumulation of KaiC at the late stage of the phosphohrylation period, which leads to molecular synchronization in the model. However, there is no mechanism of collective shift of population from the T to the R state in the ZLAW model, and hence, the oscillation of the mixture may not be entrained to the R states. With the model of Mori et al. (39), only the shuffling reactions of $R + R \rightarrow R + R$ and $T + T \rightarrow T + T$ are allowed, so there is no mechanism of collective shift of population from T to R. Hence, it may be difficult to explain the observed entrainment to the R states using the Mori et al. model. In the model of Rust et al. (27), on the other hand, the population accumulates at the last stage of the phosphorylation period and is then collectively transformed to the early stage of the dephosphorylation period. The Rust et al. model may therefore be able to explain the oscillator synchronization (34). The basic assumptions in the Rust et al. model are in contradiction to the interpretation of the experimental data of phosphomimetic mutants (26,34). However, the behavior of these phosphomimetic mutants might be different from that of phosphoforms of wild-type KaiC (34), so a further careful check is necessary for the Rust et al. model. We also note that the AMS, Rust et al., and ZLAW mechanisms may not exclude each other but may coexist to sustain stable oscillation.

Synchronization among KaiC hexamers not only should be a necessary condition for realizing collective oscillation in the reconstituted system in vitro, but also should have biological implications in vivo (41). Since a cell cultivated in constant light divides more than two times per day (47), the Kai proteins newly synthesized during cell growth and division should perturb the circadian oscillation. However, this perturbation does not damp the KaiC oscillation; instead, the amplitude and oscillation period under the constant-light condition were observed to be similar to those in the stationary phase (47) or under the constant-dark condition (23). The mechanism examined in the simulated and experimentally observed oscillator synchronization should play a major role in synchronizing the oscillation of newly synthesized Kai molecules on the whole-cell scale, so that more precise modeling of KaiC oscillation in vitro would provide a further clue to the robustness and stability of in vivo circadian oscillation.

SUPPORTING MATERIAL

One table and two figures are available at http://www.biophysj.org/biophysj/supplemental/S0006-3495(10)00314-0.

REFERENCES

1. Ishiura, M., S. Kutsuna, …, T. Kondo. 1998. Expression of a gene cluster kaiABC as a circadian feedback process in cyanobacteria. *Science*. 281:1519–1523.
2. Nakahira, Y., M. Katayama, …, T. Kondo. 2004. Global gene repression by KaiC as a master process of prokaryotic circadian system. *Proc. Natl. Acad. Sci. USA*. 101:881–885.
3. Bell-Pedersen, D., V. M. Cassone, …, M. J. Zoran. 2005. Circadian rhythms from multiple oscillators: lessons from diverse organisms. *Nat. Rev. Genet*. 6:544–556.

4. Nakajima, M., K. Imai, …, T. Kondo. 2005. Reconstitution of circadian oscillation of cyanobacterial KaiC phosphorylation in vitro. *Science*. 308:414–415.
5. Iwasaki, H., Y. Taniguchi, …, T. Kondo. 1999. Physical interactions among circadian clock proteins KaiA, KaiB and KaiC in cyanobacteria. *EMBO J*. 18:1137–1145.
6. Nishiwaki, T., H. Iwasaki, …, T. Kondo. 2000. Nucleotide binding and autophosphorylation of the clock protein KaiC as a circadian timing process of cyanobacteria. *Proc. Natl. Acad. Sci. USA*. 97:495–499.
7. Kitayama, Y., H. Iwasaki, …, T. Kondo. 2003. KaiB functions as an attenuator of KaiC phosphorylation in the cyanobacterial circadian clock system. *EMBO J*. 22:2127–2134.
8. Nishiwaki, T., Y. Satomi, …, T. Kondo. 2004. Role of KaiC phosphorylation in the circadian clock system of *Synechococcus elongatus* PCC 7942. *Proc. Natl. Acad. Sci. USA*. 101:13927–13932.
9. Iwasaki, H., T. Nishiwaki, …, T. Kondo. 2002. KaiA-stimulated KaiC phosphorylation in circadian timing loops in cyanobacteria. *Proc. Natl. Acad. Sci. USA*. 99:15788–15793.
10. Xu, Y., T. Mori, …, C. H. Johnson. 2004. Identification of key phosphorylation sites in the circadian clock protein KaiC by crystallographic and mutagenetic analyses. *Proc. Natl. Acad. Sci. USA*. 101: 13933–13938.
11. Mori, T., S. V. Saveliev, …, C. H. Johnson. 2002. Circadian clock protein KaiC forms ATP-dependent hexameric rings and binds DNA. *Proc. Natl. Acad. Sci. USA*. 99:17203–17208.
12. Hayashi, F., H. Suzuki, …, M. Ishiura. 2003. ATP-induced hexameric ring structure of the cyanobacterial circadian clock protein KaiC. *Genes Cells*. 8:287–296.
13. Williams, S. B., I. Vakonakis, …, A. C. LiWang. 2002. Structure and function from the circadian clock protein KaiA of *Synechococcus elongatus*: a potential clock input mechanism. *Proc. Natl. Acad. Sci. USA*. 99:15357–15362.
14. Vakonakis, I., J. Sun, …, A. C. LiWang. 2004. NMR structure of the KaiC-interacting C-terminal domain of KaiA, a circadian clock protein: implications for KaiA-KaiC interaction. *Proc. Natl. Acad. Sci. USA*. 101:1479–1484.
15. Garces, R. G., N. Wu, …, E. F. Pai. 2004. Anabaena circadian clock proteins KaiA and KaiB reveal a potential common binding site to their partner KaiC. *EMBO J*. 23:1688–1698.
16. Vakonakis, I., and A. C. LiWang. 2004. Structure of the C-terminal domain of the clock protein KaiA in complex with a KaiC-derived peptide: implications for KaiC regulation. *Proc. Natl. Acad. Sci. USA*. 101:10925–10930.
17. Xu, Y., T. Mori, and C. H. Johnson. 2003. Cyanobacterial circadian clockwork: roles of KaiA, KaiB and the kaiBC promoter in regulating KaiC. *EMBO J*. 22:2117–2126.
18. Ye, S., I. Vakonakis, …, J. C. Sacchettini. 2004. Crystal structure of circadian clock protein KaiA from *Synechococcus elongatus*. *J. Biol. Chem*. 279:20511–20518.
19. Uzumaki, T., M. Fujita, …, M. Ishiura. 2004. Crystal structure of the C-terminal clock-oscillator domain of the cyanobacterial KaiA protein. *Nat. Struct. Mol. Biol*. 11:623–631.
20. Pattanayek, R., D. R. Williams, …, M. Egli. 2006. Analysis of KaiA-KaiC protein interactions in the cyano-bacterial circadian clock using hybrid structural methods. *EMBO J*. 25:2017–2028.
21. Iwase, R., K. Imada, …, M. Ishiura. 2005. Functionally important substructures of circadian clock protein KaiB in a unique tetramer complex. *J. Biol. Chem*. 280:43141–43149.
22. Hitomi, K., T. Oyama, …, E. D. Getzoff. 2005. Tetrameric architecture of the circadian clock protein KaiB. A novel interface for intermolecular interactions and its impact on the circadian rhythm. *J. Biol. Chem*. 280:19127–19135.
23. Tomita, J., M. Nakajima, …, H. Iwasaki. 2005. No transcription-translation feedback in circadian rhythm of KaiC phosphorylation. *Science*. 307:251–254.
24. Akiyama, S., A. Nohara, …, Y. Maéda. 2008. Assembly and disassembly dynamics of the cyanobacterial periodosome. *Mol. Cell*. 29: 703–716.
25. Kageyama, H., T. Nishiwaki, …, T. Kondo. 2006. Cyanobacterial circadian pacemaker: Kai protein complex dynamics in the KaiC phosphorylation cycle in vitro. *Mol. Cell*. 23:161–171.
26. Nishiwaki, T., Y. Satomi, …, T. Kondo. 2007. A sequential program of dual phosphorylation of KaiC as a basis for circadian rhythm in cyanobacteria. *EMBO J*. 26:4029–4037.
27. Rust, M. J., J. S. Markson, …, E. K. O'Shea. 2007. Ordered phosphorylation governs oscillation of a three-protein circadian clock. *Science*. 318:809–812.
28. Terauchi, K., Y. Kitayama, …, T. Kondo. 2007. ATPase activity of KaiC determines the basic timing for circadian clock of cyanobacteria. *Proc. Natl. Acad. Sci. USA*. 104:16377–16381.
29. Murakami, R., A. Miyake, …, M. Ishiura. 2008. ATPase activity and its temperature compensation of the cyanobacterial clock protein KaiC. *Genes Cells*. 13:387–395.
30. Mehra, A., C. I. Hong, …, P. Ruoff. 2006. Circadian rhythmicity by autocatalysis. *PLOS Comput. Biol*. 2:e96.
31. Clodong, S., U. Dühring, …, M. Kollmann. 2007. Functioning and robustness of a bacterial circadian clock. *Mol. Syst. Biol*. 3:90.
32. Kurosawa, G., K. Aihara, and Y. Iwasa. 2006. A model for the circadian rhythm of cyanobacteria that maintains oscillation without gene expression. *Biophys. J*. 91:2015–2023.
33. Miyoshi, F., Y. Nakayama, …, M. Tomita. 2007. A mathematical model for the Kai-protein-based chemical oscillator and clock gene expression rhythms in cyanobacteria. *J. Biol. Rhythms*. 22:69–80.
34. Markson, J. S., and E. K. O'Shea. 2009. The molecular clockwork of a protein-based circadian oscillator. *FEBS Lett*. 583:3938–3947.
35. Takigawa-Imamura, H., and A. Mochizuki. 2006. Predicting regulation of the phosphorylation cycle of KaiC clock protein using mathematical analysis. *J. Biol. Rhythms*. 21:405–416.
36. van Zon, J. S., D. K. Lubensky, …, P. R. ten Wolde. 2007. An allosteric model of circadian KaiC phosphorylation. *Proc. Natl. Acad. Sci. USA*. 104:7420–7425.
37. Yoda, M., K. Eguchi, …, M. Sasai. 2007. Monomer-shuffling and allosteric transition in KaiC circadian oscillation. *PLoS One*. 2:e408.
38. Eguchi, K., M. Yoda, …, M. Sasai. 2008. Mechanism of robust circadian oscillation of KaiC phosphorylation in vitro. *Biophys. J*. 95:1773–1784.
39. Mori, T., D. R. Williams, …, C. H. Johnson. 2007. Elucidating the ticking of an in vitro circadian clockwork. *PLoS Biol*. 5:841–853.
40. Emberly, E., and N. S. Wingreen. 2006. Hourglass model for a protein-based circadian oscillator. *Phys. Rev. Lett*. 96:038303.
41. Ito, H., H. Kageyama, …, T. Kondo. 2007. Autonomous synchronization of the circadian KaiC phosphorylation rhythm. *Nat. Struct. Mol. Biol*. 14:1084–1088.
42. Monod, J., J. Wyman, and J. P. Changeux. 1965. On the nature of allosteric transitions: a plausible model. *J. Mol. Biol*. 12:88–118.
43. Perutz, M. F., A. J. Wilkinson, …, G. G. Dodson. 1998. The stereochemical mechanism of the cooperative effects in hemoglobin revisited. *Annu. Rev. Biophys. Biomol. Struct*. 27:1–34.
44. Yifrach, O., and A. Horovitz. 1995. Nested cooperativity in the ATPase activity of the oligomeric chaperonin GroEL. *Biochemistry*. 34: 5303–5308.
45. Horovitz, A. 1998. Structural aspects of GroEL function. *Curr. Opin. Struct. Biol*. 8:93–100.
46. Gillespie, D. T. 1977. Exact stochastic simulation of coupled chemical reactions. *J. Phys. Chem*. 81:2340–2361.
47. Kondo, T., T. Mori, …, S. S. Golden. 1997. Circadian rhythms in rapidly dividing cyanobacteria. *Science*. 275:224–227.